Communication

"Bottom-Up" Meets "Top-Down" Assembly in Nanoscale Polyoxometalate Clusters: Self-Assembly of $[PWO]^{-}$ and Disassembly to $[PWO]^{-}$

Chullikkattil P. Pradeep, De-Liang Long, Carsten Streb, and Leroy Cronin

J. Am. Chem. Soc., **2008**, 130 (45), 14946-14947 • DOI: 10.1021/ja806596j • Publication Date (Web): 21 October 2008

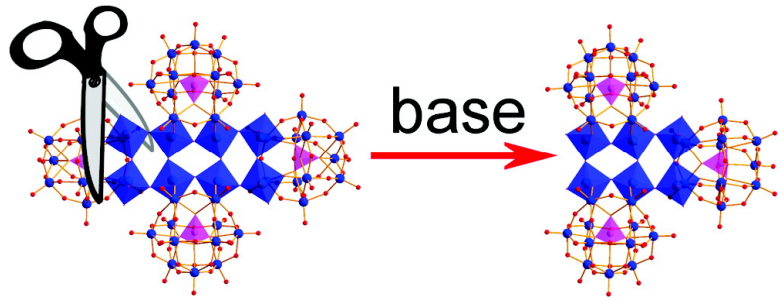

J|A|C|S
COMMUNICATIONS

Published on Web 10/21/2008

"Bottom-Up" Meets "Top-Down" Assembly in Nanoscale Polyoxometalate Clusters: Self-Assembly of $[P_4W_{52}O_{178}]^{24-}$ and Disassembly to $[P_3W_{39}O_{134}]^{19-}$

Chullikkattil P. Pradeep, De-Liang Long,* Carsten Streb, and Leroy Cronin*

WestCHEM, Department of Chemistry, The University of Glasgow, Glasgow G12 8QQ, U.K.

Received August 19, 2008; E-mail: longd@chem.gla.ac.uk; L.Cronin@chem.gla.ac.uk

Polyoxometalates (POMs) are anionic oxide clusters of early transition metals Mo, W, V, Nb, Ta, etc. with unmatched structural versatility[1] combined with applications in diverse areas such as biology[2] and catalysis.[3] The mechanism of formation of POMs is not understood, although it is generally accepted that this involves the condensation of $\{MO_x\}$units under aqueous acidic conditions. As such, nanoscale POM clusters are often synthesized starting from corresponding metal salts in a "one-pot" synthesis. Indeed, many giant POM clusters having complex structural features are synthesized by this deceptively simple, yet efficient synthetic approach.[4] The building block strategy, which utilizes the preformed lacunary clusters to build giant POM assemblies, is also well established,[5] but the reverse of these methods, i.e., the controlled decomposition of a preformed large cluster into new smaller cluster types, has not been explored systematically.[6] We are interested in developing this approach since this could serve as a powerful new route to assemble complex nanostructures that use a combination of self-assembly ("bottom-up") and partial disassembly ("top-down") to arrive at new nanoscale functional architectures as well as help identify the real building blocks present in solution during assembly.

Herein we report the synthesis and structural characterization of a large 2.65 nm phosphotungstate, $K_{24}[P_4W_{52}O_{178}]\cdot 47H_2O$ (**1**), and the pH-controlled decomposition of this parent POM into smaller phosphotungstates, $K_{20}[P_4W_{44}O_{152}]\cdot 48H_2O$ (**2**), $K_{14}[P_2W_{19}O_{69}(OH_2)]\cdot 24H_2O$ (**3**), and $K_{19}[P_3W_{39}O_{134}]\cdot 30H_2O$ (**4**) (with the cluster anions found in compounds **1**−**4** abbreviated hereafter as $\{P_4W_{52}\}$ (**1a**), $\{P_4W_{44}\}$ (**2a**), $\{P_2W_{19}\}$ (**3a**), and $\{P_3W_{39}\}$ (**4a**), respectively). $\{P_4W_{52}\}$ was initially discovered as a side product during the synthesis of $K_7[H_4P_1W_{18}O_{62}]\cdot 18H_2O$[7] but was optimized if Na_3PO_4 was used instead of H_3PO_4 as the phosphate source. Therefore, we found that reaction of $Na_2WO_4\cdot 2H_2O$ and Na_3PO_4 in 15:1 molar ratio under aqueous acidic reflux conditions (pH 1.8), followed by the addition of excess KCl, leads to the formation of a $\{P_4W_{52}\}$ cluster, which was obtained as light yellow needle-shaped crystals in 40% yield from mother liquor. Structural analysis using single-crystal X-ray crystallography revealed that the cluster present in **1** has a tetrameric structure made up of four corner-sharing $[PW_{13}O_{46}]^{9-}$ (abbreviated hereafter as $\{PW_{13}\}$) subunits, as shown in Figure 1. These $\{PW_{13}\}$ subunits can be thought of as derived by the coordination of two corner-sharing WO_6 units to the four vacant oxygen coordination sites of monolacunary α-$\{PW_{11}\}$ clusters (the boron analogue of this rare Keggin derivative has been reported as a building block in the borotungstate cluster[8] $[H_6B_3W_{39}O_{132}]^{15-}$). The corner-sharing self-assembly of four $\{PW_{13}\}$ subunits in **1** leads to the formation of a unique ladder-shaped $\{W_8O_{38}\}$ core at the center of the molecule, highlighted in blue polyhedra in its crystal structure (see Figure 1). Upon close inspection, one can find two distinct linking modes between the four $\{PW_{13}\}$ subunits in **1**. The central cluster core is assembled by a face-to-face arrangement of two $\{PW_{13}\}$ units through corner-sharing of WO_6 octahedra. Two peripheral $\{PW_{13}\}$ units are connecting to the central core in a side-on fashion, again through corner-sharing of WO_6 units. In **1a**, the former two $\{PW_{13}\}$ subunits can be termed "central" and the latter two as "peripheral" (see Supporting Information). In the molecular structure of **1**, the "central" and "peripheral" $\{PW_{13}\}$ subunits are projecting toward opposite directions about the plane of the ladder-shaped $\{W_8O_{38}\}$ core, giving rise to a "distorted nest"-shaped geometry. The result of this cross-shaped arrangement of the four $\{PW_{13}\}$ subunits is a cluster with C_2 symmetry and dimensions of approximately 2.18 × 2.65 nm; to the best of our knowledge, the cluster found in **1** represents the largest phosphotungstate reported so far in the literature,[9] as well as the largest POM cluster assembly derived exclusively from monolacunary-based building blocks.

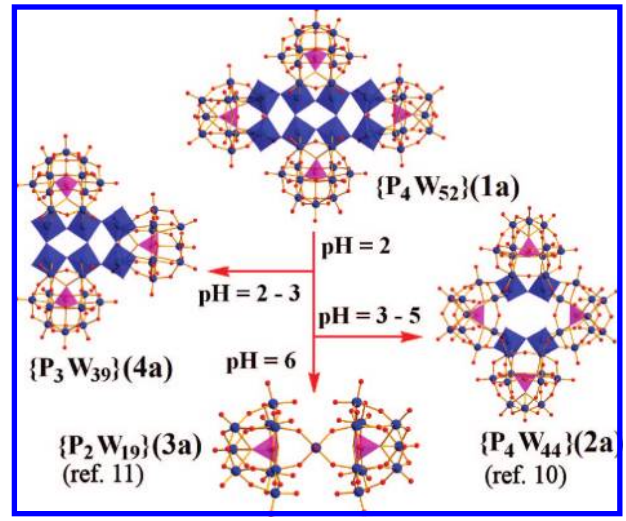

Figure 1. Molecular structures of $\{P_4W_{52}\}$ cluster anion and its pH-controlled decomposition products.

The structural asymmetry of **1a**, based on the mode of connectivity of $\{PW_{13}\}$ subunits, prompted us to explore the possibility of breaking the "loosely bound" peripheral $\{PW_{13}\}$ subunits away from the parent cluster, resulting in new smaller clusters. To test this possibility, a series of "recrystallization" experiments in the range of pH 1−7 was conducted in the presence of excess KCl. Immediate precipitation was observed at extreme pH values 1 and 7. All other solutions were clear and gave crystals after standing for 2 days. The crystals formed were collected after 5 days and structurally analyzed. It was found that the solution kept at pH 2 yielded crystals of the parent phosphotungstate $\{P_4W_{52}\}$ (**1a**) in ∼80% yield, whereas the solutions kept at pH 3, 4, and 5 gave crystals of a structurally related smaller phosphotungstate $\{P_4W_{44}\}$ (**2a**) as the product in decreasing yields (∼30% at pH 3 and ∼13% at pH 5). Interestingly, the parent cluster **1a** undergoes drastic structural changes at pH 6 and gave a much smaller cluster $\{P_2W_{19}\}$ (**3a**) (∼80% yield) under these experimental conditions. This

10.1021/ja806596j CCC: $40.75

experiment clearly proves that the parent phosphotungstate $\{P_4W_{52}\}$ can be subjected to controlled decomposition as a function of pH, resulting in new smaller cluster types.

Single-crystal X-ray analysis of cluster **2a** revealed that it is made up of two $\{PW_{13}\}$ subunits as well as two trilacunary A-α-$\{PW_9\}$ units linked alternatingly to give a crown-shaped structure as shown in Figure 1.[10] The most important structural feature of this new cluster, compared to the parent cluster, is the replacement of two $\{PW_{13}\}$ subunits with two A-α-$\{PW_9\}$ units. The central $\{W_8O_{38}\}$ core of **1a** is missing in **2a**, and the presence of the A-α-$\{PW_9\}$ unit helps it to adopt a more open crown-shaped structure, different from the closed structure of **1a**. The isolation of this new phosphotungstate **2** between pH 3 and 5 indicates that the $\{PW_{13}\}$ subunits are gradually fragmenting away from the parent phosphotungstate **1** at pH > 2. Also, some of the fragmented $\{PW_{13}\}$ units undergo further decomposition at pH > 2 to give A-α-$\{PW_9\}$ units. But above pH 5, most of the $\{PW_{13}\}$ subunits are converted into A-α-$\{PW_9\}$ and hence give rise to the phosphotungstate $K_{14}[P_2W_{19}O_{69}(OH_2)]\cdot 24H_2O$ (**3**) isolated at pH 6.[11] From the decreasing yields of $\{P_4W_{44}\}$ obtained in the pH range 3−5, it can be concluded that the amount of $\{PW_{13}\}$ subunit is gradually decreasing in solutions, with a simultaneous increase in the amount of A-α-$\{PW_9\}$ as the pH is adjusted from 3 to 5. This continues until pH 6, where $\{PW_{13}\}$ no longer exists in large concentrations, as proved by the formation of $\{P_2W_{19}\}$ as the crystalline product in high yields (see Supporting Information).

The above experiments show that the actual fragmentation and reorganization of phosphotungstate **1**, leading to the $\{P_4W_{52}\} \rightarrow \{P_4W_{44}\}$ transformation, take place mainly between pH 2 and 3. Hence, we decided to analyze the pH range 2−3 more closely and did some "recrystallization" experiments as described above in the pH range 2−3 (i.e., at pH values 2.2, 2.4, 2.6, and 2.8). We were able to isolate two new crystalline forms, very thin needle-shaped crystals and flat thin square crystals, from solutions kept at pH > 2.4 (yield ∼30%). Both of these crystals, on structural analysis, revealed a hitherto unknown phosphotungstate type, $K_{19}[P_3W_{39}O_{134}]\cdot 30H_2O$ (**4**). The structure of **4a** is made up of three $\{PW_{13}\}$ units, connected through corner-sharing, giving a final structure that appears as if one peripheral $\{PW_{13}\}$ subunit of the parent phosphotungstate **1a** is cleaved off (see Figure 1). The rest of the structural features of **4a** are quite similar to those of **1**, and it can be seen that the structure of **4a** is not symmetrical, as the three $\{PW_{13}\}$ subunits are not disposed symmetrically around the central core as observed in the analogous boron cluster[8] $[H_6B_3W_{39}O_{132}]^{15-}$. Also, it is intriguing to note that this structurally asymmetric cluster crystallizes in two crystal morphologies as needles and flat thin square crystals. We can assume that this new cluster, **4a**, is a stable intermediate in the $\{P_4W_{52}\} \rightarrow \{P_4W_{44}\}$ transformation process in the pH range 2−3.

Preliminary dynamic light scattering (DLS) measurements were used to see if transformation of $\{P_4W_{52}\}$ into smaller clusters could be seen in solution by monitoring the particle size of **1a** in solutions as a function of pH. It was found that the hydrodynamic diameter of the particles showed a gradual decrease in size as the pH of the solution was increased from 2 to 6 (from 1.7 nm at pH 2 to 0.7 nm at pH 6; see Figure 2). Although these are preliminary results, it is intriguing that the DLS data show that cluster **1a**, $\{P_4W_{52}\}$, fragments into smaller clusters with increase in pH, and this is consistent with our synthetic, structural, and analytical studies. DLS

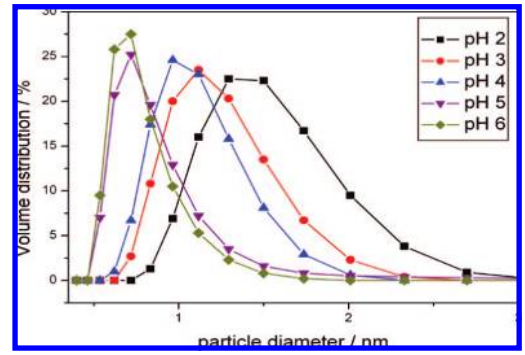

Figure 2. Volume size distribution of particles of $\{P_4W_{52}\}$ (**1a**) in solutions at different pH values using DLS (see Supporting Information).

experiments also pointed to the possibility that higher aggregations of **1a** may form, similar to the super macroions observed by Liu[12] (see Supporting Information).

In conclusion, we have reported the synthesis and structure of a nanoscale phosphotungstate, $K_{24}[P_4W_{52}O_{178}]\cdot 47H_2O$ (**1**), which is the largest phosphotungstate reported so far, and the pH-controlled decomposition of this phosphotungstate into smaller clusters with disassembly to $K_{19}[P_3W_{39}O_{134}]\cdot 30H_2O$ (**4**). Through this work, we have shown that the controlled decomposition of large POM clusters is possible, leading to the formation of new cluster types. Although one can expect the disintegration of large POM clusters under unfavorable reaction conditions, a systematic study of such a cluster decomposition process leading to the isolation and characterization of end products as well as possible intermediates is quite unprecedented. Further work will focus on the "reverse building block" approach to develop a new synthetic strategy based upon the assembly disassembly paradigm presented here, as well as expanding our solution studies to more extensive scattering and embarking upon cryospray mass spectrometry studies to better understand the disassembly process.

Acknowledgment. This work was supported by the EPSRC and The University of Glasgow and WestCHEM.

Supporting Information Available: Experimental details, including the synthesis and characterization; X-ray crystallographic (CIF) files. This material is available free of charge via the Internet at http://pubs.acs.org.

References

(1) Long, D.-L.; Burkholder, E.; Cronin, L. *Chem. Soc. Rev.* **2007**, *36*, 105.
(2) Hasenknopf, B. *Front. Biosci.* **2005**, *10*, 275.
(3) Vasylyev, M. V.; Neumann, R. *J. Am. Chem. Soc.* **2004**, *126*, 884. Mbomekalle, I. M.; Keita, B.; Nadjo, L.; Berthet, P.; Hardcastle, K. I.; Hill, C. L.; Anderson, T. M. *Inorg. Chem.* **2003**, *42*, 1163.
(4) Müller, A.; Beckmann, E.; Bögge, H.; Schmidtmann, M.; Dress, A. *Angew. Chem., Int. Ed.* **2002**, *41*, 1162. Müller, A.; Shah, S. Q. N.; Bögge, H.; Schmidtmann, M. *Nature* **1999**, *397*, 48, and references therein.
(5) Müller, A.; Peters, F.; Pope, M. T.; Gatteschi, D. *Chem. Rev.* **1998**, *98*, 239.
(6) pH-controlled decomposition of clusters into lacunary species is well-known; see, for example: Contant, R. *Inorg. Synth.* **1990**, *27*, 104.
(7) Long, D.-L.; Streb, C.; Song, Y.-F.; Mitchell, S.; Cronin, L. *J. Am. Chem. Soc.* **2008**, *130*, 1830.
(8) Leclerc-Laronze, N.; Marrot, J.; Hervé, G.; Thouvenot, R.; Cadot, E. *Chem. Eur. J.* **2007**, *13*, 7234.
(9) Contant, R.; Tézé, A. *Inorg. Chem.* **1985**, *24*, 4610.
(10) Zhang, J.; Qin, C.; Wang, E.; Su, Z.; Xu, L. *Inorg. Chim. Acta* **2007**, *360*, 3376.
(11) Tourné, C. M.; Tourné, G. F. *J. Chem. Soc., Dalton Trans.* **1988**, 2411.
(12) Liu, T. *J. Am. Chem. Soc.* **2003**, *125*, 312.

JA806596J